JOURNAL OF ENGINEERING annals OF FACULTY OF ENGINEERING HUNEDOARA
Tome V (year 2007), Fascicole 2, (ISSN 1584 – 2665)

COMPUTER MODELLING OF INDUCTION HEATING COMBINED WITH EXPERIMENT

Bohumil TARABA

SLOVAK UNIVERSITY OF TECHNOLOGY, FACULTY OF MATERIALS SCIENCE AND TECHNOLOGY, TRNAVA, SLOVAK REPUBLIC

ABSTRACT:
The article deals with computer modeling of induction heating and temperature measurement on the experimental specimen surface. Next is described methodology of creation of simulation models. The problem demonstrates the use of the multi-field solver using an electromagnetic harmonic non-linear analysis stagger and a time transient heat transfer stagger. The experimental part describes execution process of experiment. Measured temperatures are statistical calculated and compared with the results of thermal field of the numerical analysis.
KEYWORDS:
induction heating, computer modeling, simulation model, multi-field analysis, temperature measuring

1. INTRODUCTION

Computer modeling of technological processes allows to follow deeper the relationship and influence of particular parameters of study process. The result is an effective task solution on minimum costs. The modeling of induction heating is formed through joining the two analyses: harmonic electro-magnetic and transient thermal. The article deals with the task solution of the induction heating by the Ansys program code. The multi-field method is presented. The results of the numerical analysis are experimentally verified at the rotation specimen.

2. THEORETICAL BASES

In induction heating process is created an alternating magnetic field, which is penetrating into billet surface. The penetration depth is defined as the distance from the billet surface at which the current density decreases exponentially to the 1/e of its value on the surface. The skin depth δ can be calculated from the relationship [2]

$$\delta = \sqrt{\frac{\rho_{el}}{\pi \mu_0 \mu_r f}}\ , [m] \qquad (1)$$

where: ρ_{el} - is the electrical resistivity, [Ω.m],
μ_0 - is the vacuum permeability, ($4\pi.10^{-7}$ H.m^{-1}),
μ_r - is the relative permeability, [-],
f - is the frequency, [Hz].
The Joule heat generated in the element is computed as [2]

$$q_v^j = \frac{1}{n}\sum_{i=1}^{n}[\rho_{el}]\{J_{t,i}\}\cdot\{J_{t,i}\}, \qquad [W.m^{-3}] \qquad (2)$$

where: q_v^j is the Joule heat per unit volume [W.m^{-3}],
n is number of integration points,
[ρ_{el}] is the eletrical resistivity matrix [Ω.m],
{$J_{t,i}$} is the total current density [A.m^{-1}] in the element at integration point i and in time t.

The temperature fields in the heated cylindrical specimen are described by Fourier-Kirchoff´s heat equation [3]

$$\frac{\partial T}{\partial t} = a(T)\left(\nabla^2 T + \frac{q_v(r)}{\lambda(T)}\right), \qquad [K.s^{-1}] \qquad (3)$$

where: a(T) is coefficient of thermal diffusivity [m^2.s^{-1}],
λ(T) is coefficient of thermal conductivity [W.m^{-1}.K^{-1}].

Both are temperature dependent. The variable r is coordinate in cylindrical coordinate system. The thirdly type of boundary condition on the specimen surface is applied through the combined heat transfer coefficient.

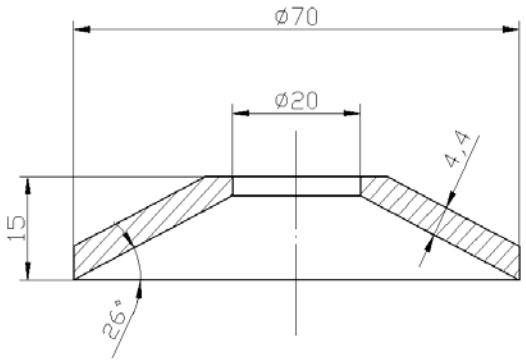

Figure 1. Geometry of specimen.

3. EXPERIMENT

For experiment was applied specimen displayed on **Figure 1**, material stainless steel EN 15CrNiSi2520. Thermocouple of type K was bonded by capacity electrical discharge on bottom specimen surface on diameter 39.4 mm.

Heating of the specimen was realized on special dedicated device AEG-ELOTHERM HF-generator type RGI 40/500 by your frequency 350 kHz and full power 50 kW. Configuration of experimental set-up was: digital thermometer GREISINGER GMH 3250 bonded with computer, specimen, inductor and siege of the device. **Figure 2** shows dimensions and design of the inductor.

The power of device was adjusted on 85 % of full power and duration of the heating was 6 second. Room temperature was 25 °C. There were executed seven measurements of temperature. The measured temperatures are shown on Figure 3.

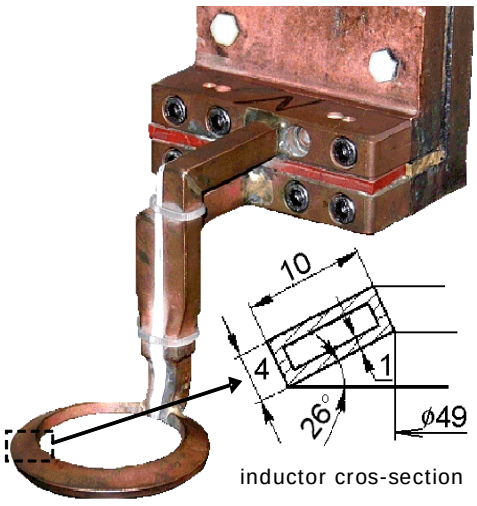

Figure 2. Inductor

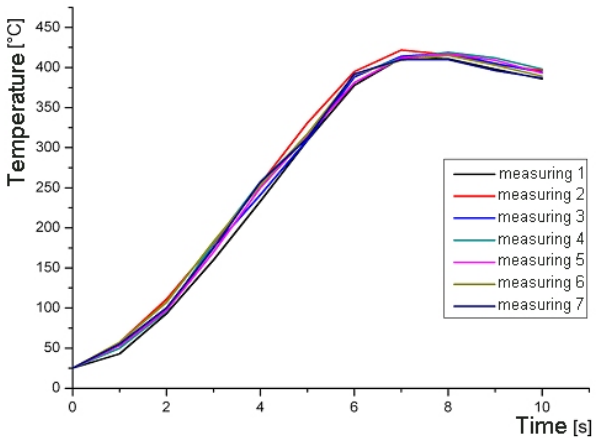

Figure 3. Measured temperatures

4. NUMERICAL SIMULATION

The solution algorithm for the ANSYS multi-field solver is shown in the **Figure 4**. The solution loop consists of three loops: field loop, stagger loop and time loop. The multi-field solver supports transient, and harmonic analysis of fields inside the field loop.

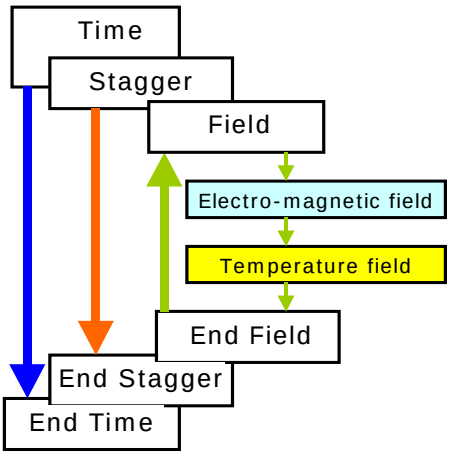

Figure 4. Solution algorithm for the ANSYS multi-field solver.

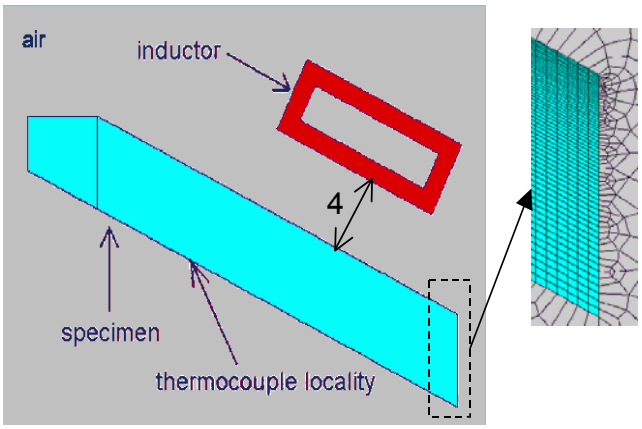

Figure 5. Geometry of simulation model with detail of generated mesh

Figure 5 shows the geometrical axisymmetric model for electromagnetic and thermal analyses with a part of generated mesh. Elements types PLANE53 and PLANE57 were used. The solution procedures were nonlinear and transient for thermal analysis. Thermo-physical properties of material **Table 1** are temperature dependent [4, 5]. The relative permeability of stainless steel is up to Curie temperature (742°C) μ_r = 1,02 [5]. The considered current density in inductor was $4.8.10^6$ A.m^{-2} [6].

Table 1. Thermo-physical properties of steel EN 15CrNiSi2520

T, [°C]	0	100	200	300	400	500	600	700
Λ [W.m^{-1}.K^{-1}]	14,8	15,8	17,0	18,4	20,0	22,0	24,0	25,7
c (specific heat) [J.kg^{-1}.K^{-1}]	455	475	495	508	525	550	572	602
ρ (density) [kg.m^{-3}]	7940	7911	7871	7830	7787	7745	7703	7662

Heat transfer from specimen surface into surrounding air was modeled by convection heat transfer with combined heat transfer coefficient (natural convection + radiation) [7]. Figure 6 shows the combined heat transfer coefficient as the function of surface temperature (emissivity of steel = 0,7 [5]).

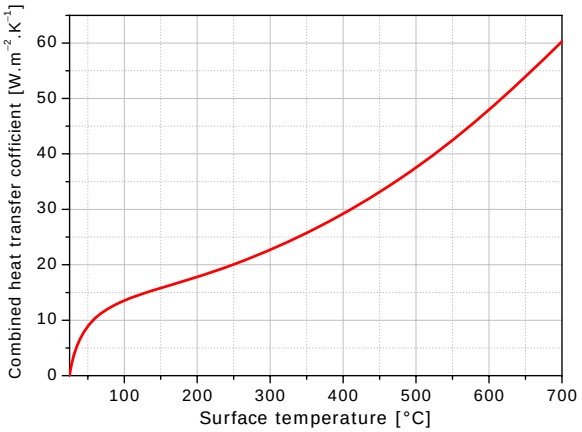

Figure 6. Combined heat transfer coefficient as the function of surface temperature

5. RESULTS OF NUMERICAL SIMULATION

In the **Figure 7** is demonstrated the magnetic field intensity value H [A.m^{-1}] between inductor and specimen. Temperature field in cross-section of specimen in time 6 sec shows **Figure 8**.

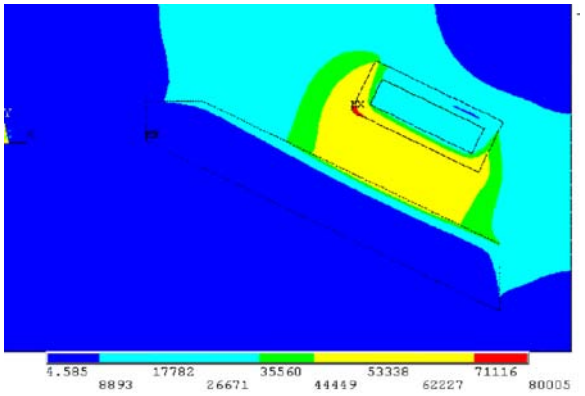

Figure 7. Magnetic field intensity H [A.m^{-1}]

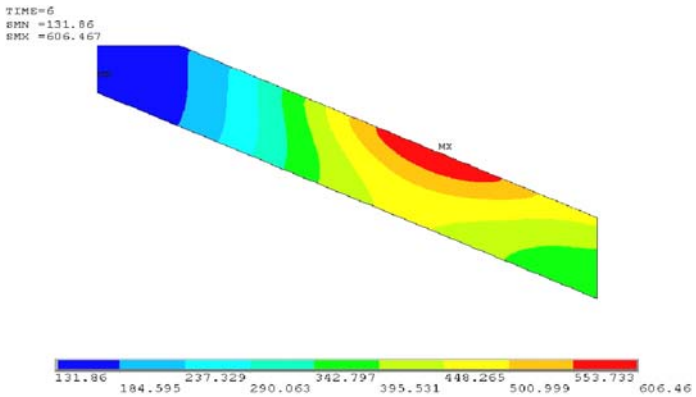

Figure 8. Temperature field [°C], time 6 sec.

Temperature time dependences in selected points of model cross-section on **Figure 9** are presented. The overlap of temperature time dependences from experiment and numerical simulation is seen on **Figure 10**.

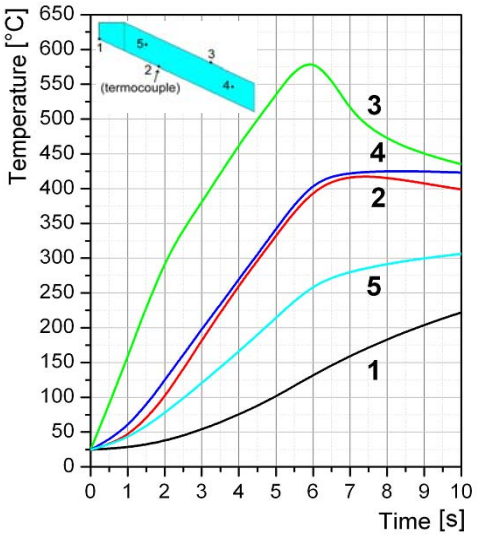

Figure 9. Temperatures in selected points

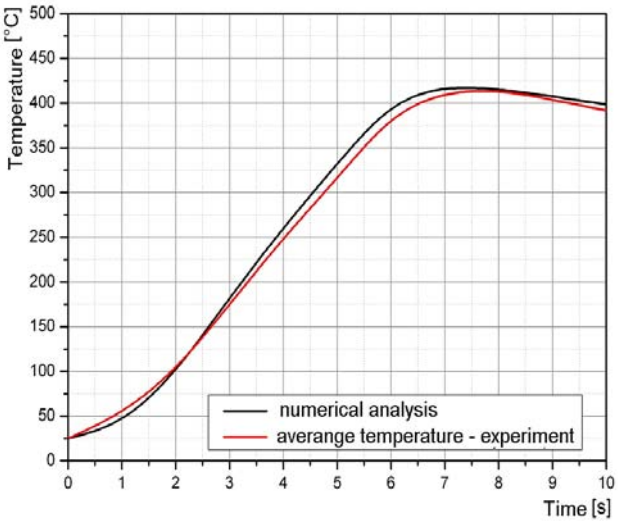

Figure 10. Comparison of temperatures from experiment and simulation

6. CONCLUSION

Results of non-linear numerical analysis of the induction heating by multi-field method showed the good-sized degree of equality with the experimental measurement. Coefficient of correlation between computed and experimental temperature is 0.9991. The correct approach by the building of simulation model returns the prediction of temperature fields with high degree of probability. Computed temperature fields are usable for stress-strain and deformation analyses.

Acknowledgements
This work is supported by the research grants of the Ministry of Education SR and Slovak Academy of Sciences VEGA 1/2101/05 and VEGA 1/2073/05.

REFERENCES

[1] ANSYS THEORETICAL MANUAL, Release 8.1, SAS IP, Inc., 2002.
[2] BEHÚLOVÁ, M.: *Numerical simulation of induction heating*. Acta Metallugica Slovaca, 11, (2005)
[3] INCROPERA, F.: *Fundamentals of Heat and Mass Transfer, 5th Ed.*. Wiley. 2001. ISBN-13 978-0471386506
[4] RADAJ D.: *Schweissprozesssimulation, Grundlagen und Anwendungen*, Verlag fur Schweissen ung Verwandte Verfaren, DVS-Verl., (1999)
[5] *www.matweb.com*, [online], [cit. 2007-6-15].
[6] DAVIES, E. D.: *Conduction and induction heating*, Inspec/Iee, London, (1989)
[7] KRAVÁRIKOVÁ, H.: *Modelling of the technological processes*. In: Academic Journal of Manufacturing Engineering. ISSN 1583-7904. - Vol. 5, No. 2 (2007)